

HARDNESS TESTING OF DIAMOND AND DIAMOND-LIKE CARBON FILMS

N.M. Everitt and A.M. Cock

Department of Aerospace Engineering, University of Bristol, Queens Building,
University Walk, Bristol BS8 1TR, UK

P.W. May, K.N. Rosser and M.N.R. Ashfold

School of Chemistry, University of Bristol, Cantock's Close, Bristol BS8 1TS, UK

The microhardness of hot filament CVD diamond films and a commercial DLC film have been tested. For the silicon and sapphire substrates investigated, the results show increased hardness even for very thin films. Indentations smaller than 10 μm can not be seen, and loads above 300g damage the indenter. The data has been compared with two models of variation in measured hardness with film thickness. One model is based on finite element analysis of indenter penetration and the other on volume fraction of deformation, but both include empirical "fitted" factors. The finite element model was more successful in predicting absolute film hardness, but both struggled to predict other physical parameters. Higher ratios of film thickness to indentation depth are needed for full validation, which may be possible using nanoindentation.

INTRODUCTION

Diamond has long been known as the hardest (natural) material, and one area of interest in diamond films is to use them as hard protective coatings. The hardness of a film might also be a screening criteria when developing growth conditions on new systems, since hardness indentation tests are easily accessible, quick to perform and only need a small sample area. However, interpretation of hardness results on any thin film system is not easy, and particularly so when the films are very hard and of varying thicknesses. In this paper we review the current models of hardness available and test out these models on hardness data obtained in our laboratory.

The ability to grow diamond at reduced pressures under metastable thermodynamic conditions, rather than high pressure synthesis, was pioneered by Spitsyn and Derjaguin (1) in the USSR and Eversole (2) in the USA. Once it was reported that chemical vapour deposition (CVD) could be carried out on non-diamond substrates (3), it has been the subject of intense research. Different methods are used to obtain the activated gas phase from which the deposition occurs, the most common of which are the use of hot filaments and microwave discharges (4). Diamond like carbon (DLC) contains diamond like bonding but is amorphous rather than crystalline.

INTERPRETATION OF INDENTATION HARDNESS DATA

Indentation Size Effects

Hardness results are often quoted as if recorded hardness is independent of load. This is not the case when using small loads (e.g. less than 200g); in fact, in general, the recorded hardness (load over projected area of the indentations) goes up as the load is decreased. This effect is referred to as the indentation size effect (ISE) and can be characterised by a Meyer index, m , where

$$P = Ad^m, \quad [1]$$

P is the applied load, A is a material constant, d is the diagonal length. If no ISE exists then $m=2$. However ISE is particularly marked in harder solids, most ceramic materials have m in the range 1.6 - 1.9 (5) and extreme in natural diamond (6). It is principally on the basis of this characteristic that genuine diamond hardness measurements over a range of values 80 to 180 GPa can be explained (7).

Film Thickness Effects

In the field of microhardness testing, in order to achieve a measured hardness which is independent of film thickness, it is conventional to have a ratio of film thickness (t) to indentation depth (h) that is 10 or more (8). However, Aisenberg and Kimock (9) claim that $t/h \geq 5$ is sufficient for DLC, whilst published results on amorphous semiconductor films show that hardness becomes independent of load at a t/h of 1.5 (10).

MODELLING HARDNESS ON THIN FILM SYSTEMS

The measured hardness of a thin film is a complicated combination of intrinsic properties (crystal structure, plastic and elastic properties) and extrinsic factors (substrate hardness, coating/substrate adhesion and film thickness etc.). How all these factors interrelate to give the final measured hardness is not well understood.

Finite Element Model

Bhattacharya and Nix (11) have used a finite element method to examine the effects of elastic and plastic properties of both film and substrate on the hardness of a film/substrate composite. Film and substrate are assumed isotropic, with no ISE effects or friction at the indenter/film interface. Equations are derived based on empirical fit of hardness versus indentation displacement data generated from finite element calculations. For the case of a hard film on softer substrate, the empirical equation is:-

$$H - H_s = (H_f - H_s) \exp \left[- \frac{H_f/H_s}{\sigma_f/\sigma_s \sqrt{E_f/E_s}} \left(\frac{h}{t} \right) \right] \quad [2]$$

where H is the hardness, E is the modulus, σ is the yield stress, t is the film thickness and h represents the total indentation displacement. The subscripts f and s refer to film and substrate respectively.

From Eq. [2], a plot of $\ln(H - H_s)$ against h/t is linear with an intercept $\ln(H_f - H_s)$. Therefore if H_s is known, H_f can be calculated.

Volume Fraction Model

An alternative method of modelling the hardness of thin film systems is to attempt to separate out the contributions to measured hardness from the film and from the substrate. The model must be based on some assumed geometry of deformation, and the contributions to hardness based on a weighted average of either volumes or areas affected by the indenter.

A volume fraction approach was initially proposed by Sargent (12). This model stated that the measured hardness was given by:-

$$H = \frac{H_f V_f + H_s V_s}{V_f + V_s} \quad [3]$$

where the volume of plastically deformed material in the film is V_f and in the substrate is V_s . The total volume of plastic deformation (V_{total}) = $V_f + V_s$.

This was subsequently modified by Burnett and Rickerby (5, 13) to include an empirically derived parameter, χ , which accounted for the deviation of plastic zone size from an idealized geometry. Using this factor, Eq. [3] can be rewritten (5,13) for hard films on soft substrates:-

$$H = \frac{H_f V_f + \chi^3 H_s V_s}{V_f + \chi^3 V_s} \quad [4]$$

χ can be approximated by

$$\chi = \left(\frac{E_f H_s}{H_f E_s} \right)^n \quad [5]$$

based on the premise that this determines the relative size of plastic zones in the two materials (14). Empirically, Bull and Rickerby found that n was usually of the order of 1/3 - 1/2 (14).

Fabes et al. (15) adapted Eq. [4] to take account of whether the indenter and its associated plastic strain field is entirely contained in the film (relevant to nanoindentation), or have penetrated the substrate. They assume the plastically deformed volume to be a 45° triangular cone, and argue that an extra volume term, V_{sd} , is required if the indenter fully penetrates the film, associated with the substrate material deformed directly by the indenter. Thus

$$H = \frac{H_f V_f + \chi^3 H_s (V_s + V_{sd})}{V_f + \chi^3 (V_s + V_{sd})} \quad [6]$$

where $V_{sd} = 0$ as long as indentation depth, h , is $< t$, and $V_s = 0$ if the radius of the cone $< t$.

Rewriting Eq. [6], gives a linear plot of H against $(H - H_s)(V_s + V_{sd})/V_f$, with intercept H_f .

EXPERIMENTAL METHODS

The diamond films were grown at Bristol by hot filament chemical vapour deposition (HFCVD) with Ta filament. The growth conditions used a gas mixture of $CH_4:H_2$, ratio 1:100, with a total flow rate of 200 sccm, at 30 Torr. The substrates investigated were single crystal (100) Si, single crystal sapphire (0112) and epitaxially grown Si on sapphire (SOS). The substrates were pre-abraded with diamond powder (1-3 μm), and their temperature during deposition is estimated to be 750°C. Deposition time varied from 0.5 to 13 hours, with a growth rate of 0.5 $\mu m/h$. Laser Raman analysis of films grown under these conditions has indicated that they are diamond, with no graphitic signal (16).

The films were hardness tested with a Matsuzawa Seiko microhardness tester using a Knoop indenter with 15 s load time. The indents' long diagonals were measured

on a optical microscope, using Nomarski interference contrast. (For the elongated pyramidal Knoop indenter, H (GPa) = $139.55 P/d^2$ where P is the applied load (g) and d is the long diagonal (μm)).

The smallest indentations that could be measured with reasonable confidence were of 10-20 μms diagonal ($d=30h$). Efforts to obtain t/h ratios higher than those shown below, by using thicker films, resulted in chipped / eroded indenter tips. Using loads above 300g on diamond films resulted in significant indenter damage (17). The film thicknesses were estimated from SEM images.

RESULTS AND DISCUSSION

The materials constants used in the model predictions are shown in Table 1. These values were chosen as being generally representative of the Si substrate and diamond film, since the actual physical constants of our films or substrate are not known. The value chosen for the Young's modulus is that which has been found for microwave-plasma diamond films with low hydrogen content (18) using the vibrating reed method.

Error bars on graphs show 95% confidence limits.

Our hardness data could be fitted to the linear version of Eq. [2] (finite element model) with a correlation coefficient, R , of 0.9537, giving a confidence level of > 99.5% in the fit (see Fig. 1). The intercept value gives $H_f = 112$ GPa, which accords quite well with the hardness of bulk diamond. Using the gradient of the fitted line one of the 4 quantities E_f , E_s , σ_s or σ_f can be estimated, providing that the other 3 are known. The modulus can be relatively easily measured by vibrating reed techniques or bulge tests (18, 19, 20). If E_f , E_s and σ_s are assumed to be the values in Table 1, then the gradient of the line can be used to predict the yield stress of the film. In this case $\sigma_f = 7.9$ GPa, which is a more than a factor of 4 less than the 35 GPa calculated for bulk diamond (21).

In applying the volume fraction model in Eq. [6] we are assuming that (i) the indentation preserved the geometry of the Knoop indenter and (ii) the elastic contraction of the long diagonal is negligible and thus h includes both plastic and elastic contributions to the total deformation under load. Since the model is based on conical symmetric deformation, it was calculated what cone radius would give the projected surface area of indentation equivalent to our Knoop indentation. The linear version of Eq. [6] is shown fitted to our hardness data in Fig. 2. The fit has an R value of 0.8499, which gives a confidence level of 99%. The intercept of this line gives $H_f = 55$ GPa, which is much lower than bulk. Using the moduli and hardness values as before, an n value of 3.0 is predicted by the gradient of the plot. This is an order of magnitude above the empirical value found by Bull and Rickerby (14). Taken with the low value of predicted hardness, it would seem that the volume fraction model is less successful, at least with our data. After adding an indentation size effect factor, Burnett and Rickerby (13) were able to fit H_f and n to experimental hardness data of titanium nitride and tungsten-titanium coatings on a variety of softer substrates. However, it should be noted that the depth of indentations ($\mu\text{m}'\text{s}$) were about the same as the coating thicknesses, thus the true properties of the film hardness were only approached asymptotically as the contact depth approached 0. Physically, it does seem likely that ISE plays a part in correct modelling of hard film and substrate systems.

All the experimental data and the two best fit lines are shown in Fig. 3. One reason for the difference in H_f predictions by the two models is probably due to the discrepancies in the t/h ratio at which the measured hardness becomes independent of

hardness. As mentioned in a previous section, suggested values vary from ≥ 1.5 to ≥ 10 . The finite element model suggests that this point of load independent hardness differs depending on the hardness difference between substrate and film, and is > 100 for diamond on silicon. In contrast the volume mixture model predicts, by definition, that the hardness becomes load independent when the depth of the plastic zone is less than t . This is at $t/h = 4.6$. Unfortunately we could not obtain data up to this t/h value (see Experimental methods) but it should be possible to do so with thicker DLC films if not with diamond.

Data from diamond on sapphire and diamond on SOS (Fig. 4) also demonstrate that the substrate material(s) are still having a large effect at these lower t/h ratios, since the diamond film on SOS gives a considerably lower hardness reading than the same thickness diamond film on the sapphire wafer. The diamond film on SOS will not give a higher hardness result than the monolithic sapphire wafer until the t/h ratio is such that the plastic deformation zone is no longer incorporating the Si.

Measured hardnesses of DLC films of $0.4 - 0.5 \mu\text{m}$ thicknesses show that even when the depth of the indentation is considerably larger than the film thickness, significant difference in hardness is still recorded. It seems likely that rather than the indenter cutting through the film, a thin compressed layer remains between the indenter and the substrate. Thus the volume fraction model when the indenter penetrates the substrate at $h=t$ may not be physically correct at that point.

The measured hardness of the silicon wafers is sensibly constant over the size of indentations used, but this is not the case for sapphire (Fig. 4). This agrees with the observation that ISE effects are more pronounced with stiffer harder materials, although Burnett and Page (23) quote $m=1.7$ for Si wafers.

CONCLUSIONS

A finite element model and a volume fraction model predicting the variation of measured hardness with thin film thickness have been compared with our own data from diamond films. The empirical finite element model gave a slightly better fit to our data than the volume fraction model, but results at higher t/h ratios are needed to fully validate the model. These results will only be possible for diamond films using depth sensing nanoindentations, since microhardness indentations at low loads cannot be seen on the thicker films. However, given the rough morphology of film surfaces, such testing is problematic, and films may need to be polished first. ISE effects will need to be incorporated in any models of those data, together with load-bearing-area corrections which become more important in nanoindentations. Work is also needed on modelling the effect of the strength of the film/substrate interface, and the effect of residual stresses in the films.

ACKNOWLEDGEMENTS

This work has been carried out with the support of the Department of Trade and Industry. One of us (PWM) would also like to thank the Ramsay Memorial Trust for financial support.

REFERENCES

1. Spitsyn, B.V. and Derjaguin, B.V., *U.S.S.R. Inventors Certificate (Patent Application)*, July 10, 1956; *U.S.S.R. Patent* 339, 134 (1980).
2. W. Eversole, *U.S. Patents* 3030187, 3030188, (filed 1959) (1962).

3. B.V. Spitsyn, L.L. Bouillov, and B.V. Derjaguin, *J. Crys. Growth*, **52**, 219 (1981).
4. J.C. Angus, *Thin Solid Films* **216**, 126 (1992).
5. P.J. Burnett and D.S. Rickerby, *Thin Solid Films*, **148**, 41 (1987).
6. C.A. Brookes and E.J. Brookes, *Diamond and Related Mat.*, **1**, 13 (1991).
7. C. Brookes, in *The Properties of Natural and Synthetic Diamond*, edited by J.E. Field, p.383, Academic Press, London (1979).
8. H. Bückle, in *The Science of Hardness Testing and its Research Applications*, edited by J.W. Westbrook and H. Conrad, p. 45, American Society of Metals, Ohio (1973).
9. S. Aisenberg and F.M. Kimock, *Mat. Sci. Forum*, **52**, 1 (1989).
10. I.P. Manika, J.J. Maniks and J.A. Teteris, *J. Mat. Sci. Lett.*, **7**, 641 (1988).
11. A.K. Bhattacharya and W.D. Nix, *Int. J. Solids Structures*, **24**, 1287 (1988).
12. P.M. Sargent, in *Microindentation Techniques in Materials Science and Engineering*, edited by P.J. Blau and B.R. Lawn, American Society for Testing and Materials, Philadelphia (1986).
13. P.J. Burnett and D.S. Rickerby, *Thin Solid Films*, **148**, 51 (1987).
14. S.J. Bull and D.S. Rickerby, *Br. Ceram. Trans J.*, **88**, 77 (1989).
15. B.D. Fabes, W.C. Oliver, R.A. McKee and F.J. Walker, *J. Mater. Res.*, **7**, 3056 (1992).
16. P.W. May, N.M. Everitt, C.G. Trevor, M.N.R. Ashfold and K.N. Rosser, *submitted to Appl. Surf. Sci. January 1993*.
17. N.M. Everitt, P.W. May, K.N. Rosser, M.N.R. Ashfold and C.G. Trevor, abstract no. 13.149, *Proceedings of ICNDST-3, COMST, Lausanne* (1992).
18. Y. Seino, N. Hida and S. Nagai, *J. Mat. Sci. Lett.*, **11**, 515 (1992).
20. J.E. Field, in *the Properties of Natural and Synthetic Diamond*, edited by J.E. Field, p. 509, Academic Press, London (1992).
21. J.E. Field (Ed.), *Properties of Natural and Synthetic Diamond*. p.680, Academic Press, London (1992).
22. A.K. Bhattacharya and N.D. Nix, *In. J. Solid Structures*, **24**, 881 (1988).
23. P.J. Burnett and T.F. Page, *J. Mat. Sci.*, **19**, 845 (1984).

Table 1 Material constants used in models

	Young's Modulus (GPa)	Ref.	Yield Stress (GPa)	Ref
Diamond	960	(18)	-	
Silicon	127	(22)	4.33	(22)

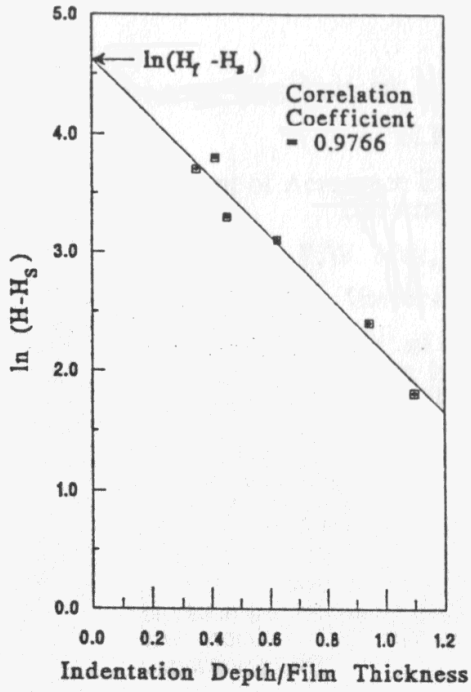


Fig. 1. Best fit line for finite element model using data from diamond films.

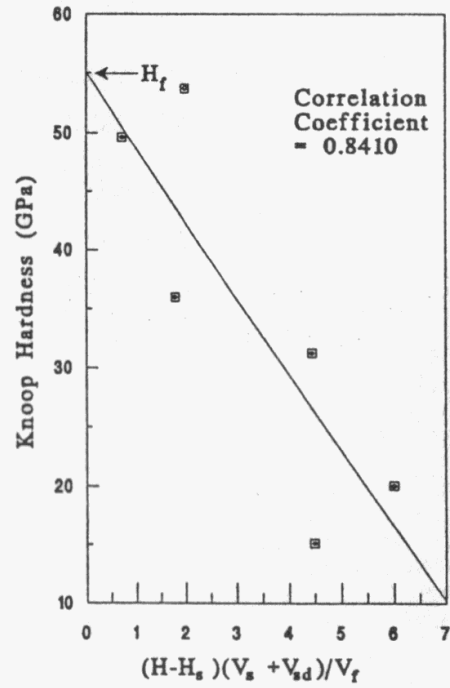


Fig. 2. Best fit line for volume fraction model using data from diamond films.

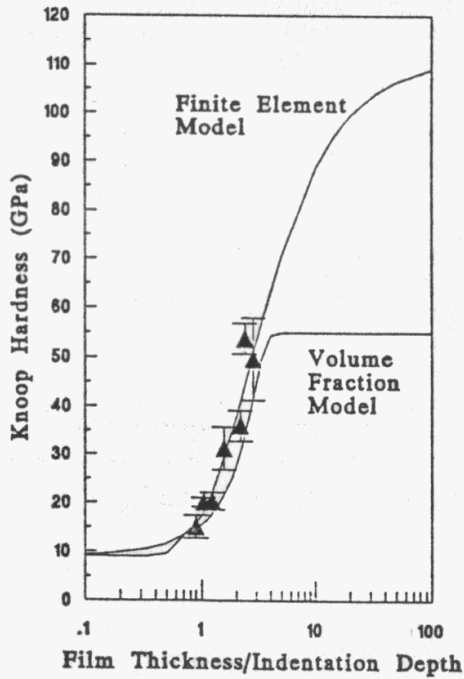


Fig. 3. Comparison of best fit lines using hardness data from diamond films.

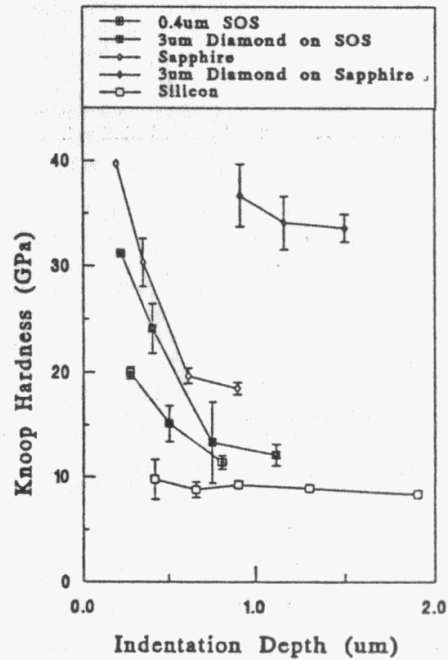


Fig. 4. Hardness of a variety of substrates at different loads.